Research Paper

Mechanistic Study of the Effects of Different Dosages of Gemcitabine on the Migratory and Invasive Abilities of Lung Adenocarcinoma A549 Cells

MENG WANG, DI QIAO AND QIANG WANG*

Department of Cardiothoracic Surgery, Shanghai Pudong New Area Zhoupu Hospital, Pudong, Shanghai 201318, China

Lung adenocarcinoma is known to be a malignancy and a leading contributor to mortality. This research intended to delve into the impact of various dosages of gemcitabine on lung adenocarcinoma A549 and PC-9 cells proliferation, migration, and invasion. Additionally, the possible underlying mechanisms were also examined. An *in vitro* cell model was utilized in the experiment. Varying doses of gemcitabine (2.5, 5, 10 µM) were administered for treating A549 and PC-9 for 0 h-96 h. 3-(4,5-dimethylthiazol-2-yl)-2,5 diphenyl tetrazolium bromide determined the half-maximal inhibitory concentration of gemcitabine in A549 and PC-9. The experiment of cell counting kit-8 assayed cell proliferation and flow cytometry tracked cell apoptosis. The assay of Transwell examined cell migration and invasion. Furthermore, the analysis of Western blot gauged the profiles of apoptotic proteins c-caspase 3 and B-cell lymphoma 2-associated X protein, the anti-apoptotic protein B-cell lymphoma 2, and the Janus tyrosine kinase 2/signal transducer and activator of the transcription 3 signaling pathway in A549 and PC-9. As suggested by our findings, gemcitabine dampened proliferation, invasion, and migration while boosting apoptosis in the cells of A549 and PC-9. Further investigations unveiled that gemcitabine impeded Janus tyrosine kinase 2/signal transducer and activator of the transcription 3 signaling pathway activation in these cells. To conclude, this research has corroborated that gemcitabine exerts inhibitory effects on A549 and PC-9 cells' proliferation, invasion, and migration capabilities by repressing Janus tyrosine kinase 2/signal transducer and activator of the transcription 3 signaling pathway activation under lung adenocarcinoma conditions.

Key words: Lung adenocarcinoma, gemcitabine, Janus tyrosine kinase 2/signal transducer and activator of the transcription 3 signaling pathway, caspase 3

Lung cancer stands as a prevailing catalyst for mortality arising from cancer across the expanse of the globe[1]. Non-Small Cell Lung Cancer (NSCLC) constitutes approximately 80 %-85 % of the entire spectrum of lung cancer instances and is additionally partitioned into squamous cell carcinoma, adenocarcinoma, as well as large cell carcinoma. Amidst the array of NSCLC subcategories, Lung Adenocarcinoma (LUAD) presents the most pronounced heterogeneity and invasiveness. It is distinguished by a notably elevated tumor mutation burden pertaining to mutations in Epidermal Growth Factor Receptor (EGFR), V-Raf Murine Sarcoma Viral Oncogene Homolog B1 (BRAF), Kirsten Rat Sarcoma Viral Oncogene (KRAS), Erythroblastic Oncogene B (ERBB2), Anaplastic Lymphoma Kinase (ALK), Tumor Protein P53 (TP53), Serine/Threonine Kinase 11 (STK11), and Transthoracic Echocardiography (TTE1), representing a considerable menace to the well-being and survival of patients[2]. Presently, therapeutic approaches encompass chemotherapy, radiotherapy, immunotherapy, targeted therapy, and surgical resection. Nonetheless, on account of insufficient early detection, a significant proportion of patients are diagnosed at advanced stages, precluding surgical interventions or radical radiation therapy. Consequently, the emergence of novel treatments such as chemotherapy agents, targeted therapies, and immunotherapies has contributed to an improvement in the survival rates of lung cancer patients[3].

***Address for correspondence**
E-mail: doctor94@126.com

Gemcitabine (GEM), classified as an antimetabolite chemotherapy agent, exerts its therapeutic effects primarily by disrupting the synthesis of Deoxyribonucleic Acid (DNA) and Ribonucleic Acid (RNA) within cancer cells. Through the inhibition of cellular division and replication processes, GEM obstructs cancer cell proliferation, thereby curbing tumor growth and spreading[4]. As reported, GEM, in the context of cancer, can transform into active metabolites and upon entry into cancer cells, phosphorylates into GEM diphosphate (dFdCDP). This phosphorylated form of GEM can bind to the bases involved in DNA synthesis, thereby impeding DNA chain extension and replication, ultimately leading to cancer cell death[5]. This phenomenon has been substantiated in pancreatic cancer[6], bladder cancer[7], and breast cancer[8]. Moreover, GEM can further suppress the proliferation and survival of LUAD cells through its interplay with relevant metabolic pathways and signaling pathways[9]. Therefore, this report places emphasis on investigating the function of GEM in the biological functions of LUAD cells, while delving into its associated underlying mechanisms. These findings may hold substantial implications for the clinical treatment of LUAD.

The Janus Tyrosine Kinase (JAK)/Signal Transducer and Activator of Transcription 3 (STAT3) pathway is a widely acknowledged intracellular signaling mechanism that assumes a central position in modulating cell differentiation, apoptosis, proliferation, and invasion[10]. Amongst mammalian organisms, the JAK family consists of four integral components; JAK1, JAK2, JAK3, and Tyrosine Kinase 2 (TYK2). STAT3 belongs to the transcription factor family. Within the confines of the JAK family, JAK2 has arisen as a pivotal target for cancer treatment on account of its pivotal role in cellular growth and survival[11]. The STAT family comprises a total of seven constituents; STAT1-STAT4, STAT5a, STAT5b, and STAT6L[12]. Research indicates that the STAT family exerts a crucial function in regulating cell proliferation, death, tumor death, metastasis, etc.,[13]. STAT3 monomers were phosphorylated in the cytoplasm, dimerized into dimers, and ultimately turned into active STAT3. Activated STAT3 enters into the nucleus, where it combines with other nuclear proteins, directly modulating the profiles of tumor-regulating genes and thus influencing multiple cellular biological functions[14]. Reports suggest that STAT3 activation is linked to processes like Epithelial-Mesenchymal Transition (EMT) transformation, tumor angiogenesis, and tumor immune escape[15]. JAKs are the primary activators of STAT proteins. JAKs, initiated subsequent to tyrosine phosphorylation, recruit and phosphorylate STATs, forming homologous or heterologous phosphorylated dimers. These dimers swiftly enter the nucleus to regulate gene expression or interact with other transcription factors in the nucleus to modulate gene expression, hence regulating a series of processes like cell proliferation, apoptosis, inflammatory response, immune response, and more[16]. Therefore, agents and inhibitors targeting the JAK/STAT3 signaling pathway have emerged as a focal point of tumor research, although the correlation between GEM and JAK/STAT3 remains obscure.

This investigation explicates the function and mechanism of GEM within LUAD cells. Our investigation has the potential to enhance comprehension regarding GEM's plausible mechanisms for treating LUAD and offer novel perspectives for the clinical handling of the ailment.

MATERIALS AND METHODS

Culture and treatment of cells:

A549 and PC-9, two human NSCLC cell lines, were acquired from the cell center of the Chinese academy of sciences situated in Shanghai, China. The cells were cultivated within a Roswell Park Memorial Institute (RPMI) 1640 culture medium enriched with 10 % Fetal Bovine Serum (FBS) and 1 % penicillin/streptomycin. The cellular cultivation procedure was executed within a controlled incubator environment set (37°, 5 % Carbon dioxide (CO2)). During the stage of logarithmic growth, the cells experienced digestion and passage through the use of 0.25 % trypsin (Thermo Fisher HyClone, Utah, United States of America (USA)). As for drug treatment, A549 and PC-9 went through treatment with GEM of varying concentrations (2.5, 5, and 10 μM) for duration of 48 h.

3-(4,5-dimethylthiazol-2-yl)-2,5 diphenyl tetrazolium bromide (MTT) assay:

During the logarithmic growth stage, A549 and PC-9, subsequent to trypsinization, were made into cell suspensions (1×10^4/ml density). These

suspensions were then seeded onto 96-well plates with a culture medium supplemented with GEM (0, 10, 20, 40 and 80 µM). The culture of cells conducted then lasted 48 h. After the procedure, 20 µl of MTT solution (5 g/l) (Sigma-Aldrich, St. Louis, Missouri) was given to each well, followed by a 4 h incubation period. Next, the culture solution was meticulously withdrawn, with 150 µl of dimethyl sulfoxide introduced into each well. The plates were shaken for duration of 10 min within a dark setting to guarantee the complete dissolution of the crystal substances. At a wavelength of 490 nm, the measurement of each well's Absorbance (A) was done with the help of a microplate reader. This experimental process was replicated thrice to ensure reliability. Then, the cellular inhibition rate was computed, and the Half-Maximal Inhibitory Concentration (IC_{50}) value was derived. The formula was designed as the follows:

Cell inhibition rate (%) =1-(Optical Density (OD) value of the experimental group/OD value of the normal group)×100 %

Cell Counting Kit-8 (CCK-8) for cell proliferation examination:

A549 and PC-9 (1×10^4/ml), inoculated onto six 96-well plates, were treated with the use of GEM (2.5, 5 and 10 µM). In each group set five replicate wells, and an incubator was utilized for cell culture. Following GEM treatment for a duration of 0 h-96 h, each well was filled with 10 µl CCK-8 reagent (Hubei Biossci Biotechnology Co., Ltd.) for further incubation of 1.5 h. Next, the absorbance at 450 nm wavelength was gauged with the help of an enzyme-linked immunoassay instrument (Multiskan™ GO, Thermo, USA). The maximum and minimum values were excluded from each group, and the mean value was obtained after subtracting the blank control group's absorbance value.

Flow cytometry for apoptosis examination:

A549 and PC-9 during the phase of logarithmic growth were seeded (6×10^4 cells/ml density) onto 6-well plates. Upon approximately 50 % confluence attained by the cells, the solution in the plates was discarded. GEM (2.5, 5 and 10 µM) was administered to the wells. The cells were cultivated for 72 h running in an incubator (37°, 5 % CO_2) before being harvested. Following digestion achieved through 0.25 % trypsin without ethylenediaminetetraacetic acid, the cells underwent centrifugation (400 r/min, 5 min), with the supernatant discarded. The specific procedure was conducted as per the guidelines of the BD Annexin V-Fluorescein Isothiocyanate (FITC) Cell Apoptosis Detection Kit (Yeasen Biotech Co., Ltd.). After Ribonucleases (RNase), FITC, and Propidium Iodide (PI) were added respectively for 15 min incubation, a flow cytometer was harnessed for analyzing cell apoptosis.

Transwell for detection of migration and invasion:

Cellular migratory and invasive capacities were measured through the migration and invasion tests of Transwell. PC-9 and A549 were dispersed using 0.25 % trypsin, followed by centrifugation and resuspension. Subsequently, they were distributed into individual wells of a 24-well culture plate. In the test for examining invasion, Matrigel chambers (Corning, Beijing, China) with a pore size of 8 µm came into use, whereas the migration experiment excluded this step. Approximately 5×10^4 cells post transfection were put in the upper chamber containing Matrigel, while the lower compartment incorporated a medium enriched with FBS (10 %) in addition to RPMI-1640 (400 µl). After incubation with 48 h duration (37°), cells that did not migrate were eliminated from the upper compartment. Later, the Transwell membranes were fixed with the use of 4 % paraformaldehyde (10 min), dyed in crystal violet (0.5 %), flushed in running water, and placed under an inverted microscope for counting.

Quantitative Reverse Transcription-Polymerase Chain Reaction (qRT-PCR):

TRIzol reagent extracted total cellular RNA in accordance with the supplier's instructions (Invitrogen, Waltham, Massachusetts, USA). A Nano drop-spectrophotometer was operated for the determination of RNA concentration and purity. On the basis of the manufacturer's guidelines, 1 µg of total RNA was taken for synthesizing complementary DNA (cDNA) with the assistance of the PrimeScript™ RT kit (Madison, Wisconsin, USA). Afterwards, qRT-PCR was executed employing SYBR® Premix-Ex-Taq™ (Takara, Texas, USA) together with the ABI7300 system. The PCR system had a total volume of 30 µl, and each specimen accommodated 300 ng of cDNA.

The amplification program encompassed an initial denaturation (95°) for 10 min, followed by 45 cycles of 10 s (95°), 30 s (60°), and 20 s (85°). All fluorescence data were transformed into relative quantification. The internal reference for JAK2 and STAT3 was Glyceraldehyde 3-Phosphate Dehydrogenase (GAPDH). Each qRT-PCR reaction was duplicated thrice. The detailed sequences of the primers were as follows; JAK2 forward primer: 5′-TCATAACCTGGAGACCCT-3′, reverse primer: 5′-ATGTTTCCCTCTTGACCAC-3′; STAT3 forward primer: 5′-TAACATTCTGGGCACGAACA-3′, reverse primer: 5′-GGCATCAATTGGCACGG-3′ and GAPDH forward primer: 5′-CCACTCACCTGCTGCTACTCATTC-3′, Reverse primer: 5′-CTGCTGGTGATCCTCTTGTAG-3′.

Western blot:

The total cellular protein from each cohort was extracted, with the bicinchoninic acid assay technique adopted for the evaluation of the protein concentration. The extracted protein was stored at -80° for later use. After denaturation, 20 µg of the protein was loaded per well and isolated through the utilization of 10 % Sodium Dodecyl Sulfate Polyacrylamide Gel Electrophoresis (SDS-PAGE). Subsequently, the protein was electro-transferred onto Polyvinylidene Difluoride (PVDF) membranes (Millipore, Bedford, Massachusetts, USA) under a 300 mA constant current. Afterwards, the PVDF membranes underwent sealing with the use of Tris-Buffered Saline with 0.1 % Tween® 20 (TBST) detergent which incorporated 5 % skimmed milk for a period of 1 h at Room Temperature (RT). The membranes went through an overnight incubation (4°) with the following primary antibodies; anti- B-Cell Lymphoma 2 (Bcl-2) (1:1000, ab59348, Abcam, Massachusetts, USA), anti- Bcl-2-Associated X Protein (BAX) (1:1000, ab32503), anti-caspase3 (1:1000, ab13847), anti-E-cadherin (Abcam, ab15148, concentration 1:1000), anti-vimentin (Abcam, ab92547, concentration 1:1000), anti-N-cadherin (Abcam, ab18203, concentration 1:1000), anti-JAK2 (Abcam, ab108596, concentration 1:1000), anti-p-JAK2 (Abcam, ab32101, concentration 1:1000), anti-STAT3 (Abcam, ab119352, concentration 1:1000), anti-p-STAT3 (Abcam, ab76315, concentration 1:1000), and anti-GAPDH (Abcam, ab8245, concentration 1:1000). After the incubation period, the membranes underwent four rinses with TBST, with each rinsing lasting 8 min. The appropriate secondary antibodies (all diluted 1:2000) were incubated at RT for 1.5 h, followed by four washes with TBST, 8 min each. The pierce enhanced chemiluminescence Western blot substrate kit from thermos was exploited for X-ray development.

Analysis of statistics:

The t-test compared statistics between the two groups. As for comparisons among various sets of data, one-way analysis of variance was exploited. Then, Tukey's post hoc test analyzed the disparity between the two groups. Statistical Package for the Social Sciences (SPSS) 24.0 (SPSS Inc., Chicago, Illinois, USA) was introduced for calculating mean±scanning electron microscopy outcomes (Mean±Standard Error of the Mean (SEM)). Graphical representations were generated through Graph Pad 8.0 software. When $p<0.05$, variances were regarded to hold statistical significance.

RESULTS AND DISCUSSION

PC-9 and A549 went through GEM (0-80 µM) stimulation for 48 h. MTT assay confirmed cytotoxicity and IC_{50} values. The chemical equation for GEM is depicted in fig. 1A. MTT unraveled that when the inhibition rate of A549 and PC-9 attained 50 %, the calculated IC_{50} values of GEM were 7.280 µM and 6.403 µM, respectively (fig. 1B and fig. 1C). Therefore, in subsequent investigations, the concentrations of 2.5, 5, and 10 µM were selected, representing low, medium, and high levels, respectively.

For the purpose of probing the impact of varying concentrations of GEM (2.5, 5, and 10 µM) on PC-9 and A549 cells' proliferation and apoptosis, the methodologies employed encompassed CCK-8 assay and flow cytometry. Given the experimental outcomes, *vs.* the group of control, higher concentrations of GEM notably abated A549 and PC-9 cells' proliferation ($p<0.05$, fig. 2A and fig. 2B) and dramatically augmented the cells apoptosis ($p<0.05$, fig. 2C and fig. 2D). Moreover, Western blot analysis confirmed that, in a concentration-dependent pattern, GEM lowered the profiles of c-caspase3 and BAX proteins while suppressing the profile of Bcl-2 protein in PC-9 and A549 by contrast with the group of control ($p<0.05$, fig. 2E

and fig. 2F). All these discoveries reflected that GEM dampened PC-9 and A549 cells' proliferation but boosted their apoptosis.

With the purpose of investigating the impact of GEM on LUAD cell metastasis, Transwell was implemented to examine their migratory and invasive capabilities, while Western blot ascertained the profiles of proteins correlated with EMT within the cells. The experimental outcomes denoted that regarding the control cohort, GEM-treated A549 and PC-9 displayed diminished migratory and invasive capacities ($p<0.05$, fig. 3A-fig. 3D). Moreover, GEM presented a dose-dependent reduction in vimentin and N-cadherin levels, while concurrently enhancing E-cadherin's profile in PC-9 and A549 ($p<0.05$, fig. 3E and fig. 3F). The above observations collectively demonstrated that GEM repressed PC-9 and A549 cells' migration, invasion, and EMT progression, thus exerting an anti-tumor effect.

With the intention of substantiating the influence of GEM on the JAK2/STAT3 pathway, A549 and PC-9 went through GEM treatment (2.5-10 μM) over a 48 h timeframe. PCR and Western blot experiments evaluated JAK2 and STAT3 mRNA and protein profiles, indicating that GEM presented a dose-dependent inhibition of JAK2 and STAT3 profiles and phosphorylation ($p<0.05$, fig. 4A-fig. 4D). All these phenomena demonstrated GEM exerted its cancer-suppressing function by dampening JAK2/STAT3 signaling pathway activation.

The cells underwent treatment with GEM (5 μM) alone or AG490+GEM for 48 h. Cell proliferation, apoptosis, and metastasis were monitored. The statistics unveiled that *vs.* the GEM group, AG490 in combination with GEM further impeded cell proliferation ($p<0.05$, fig. 5A), augmented apoptosis ($p<0.05$, fig. 5B), and dampened migration and invasion ($p<0.05$, fig. 5C and fig. 5D). The above observations substantiated that the cooperative action of AG490 and GEM suppressed A549 and PC-9 cells' proliferation, invasion, and migration while eliciting their apoptosis.

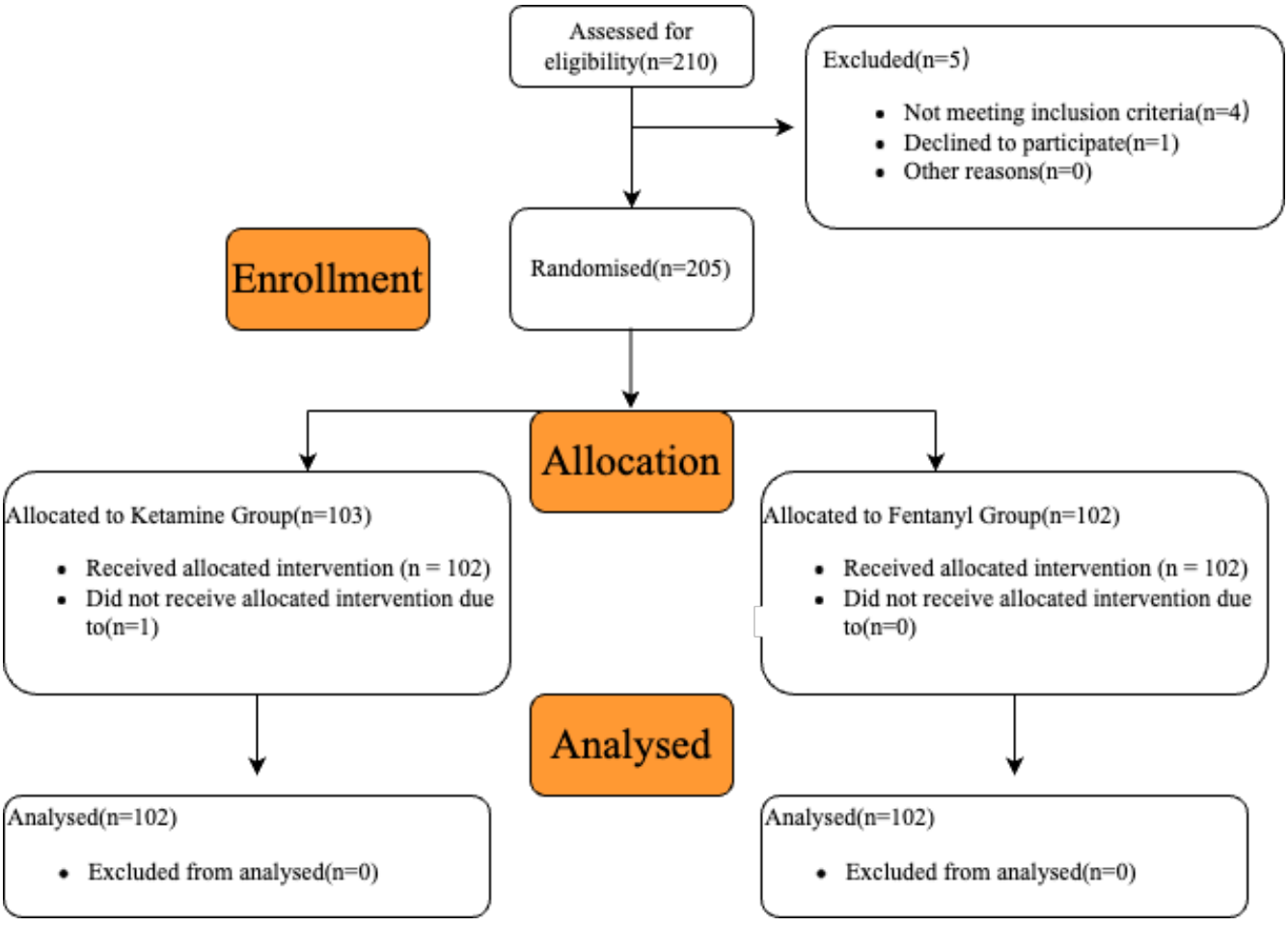

Fig. 1: Research process

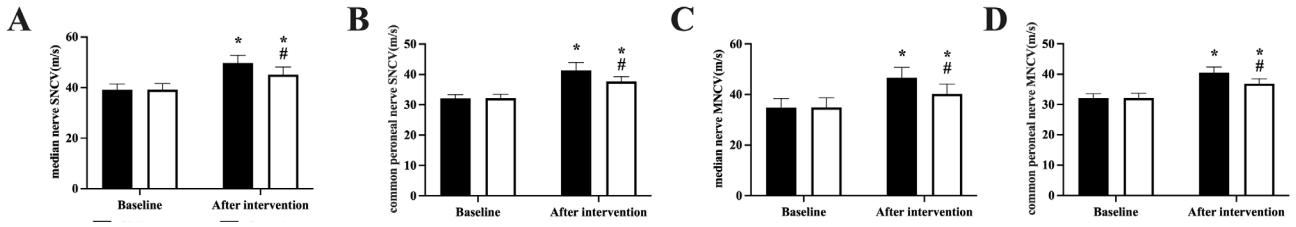

Fig. 2: Comparison of electrical nerve indices between the two groups, (A): Comparison of median nerve SNCV; (B): Comparison of common peroneal nerve SNCV; (C): Comparison of median nerve MNCV and (D): Comparison of common peroneal nerve MNCV
Note: (■): CBT group and (▭): Control group

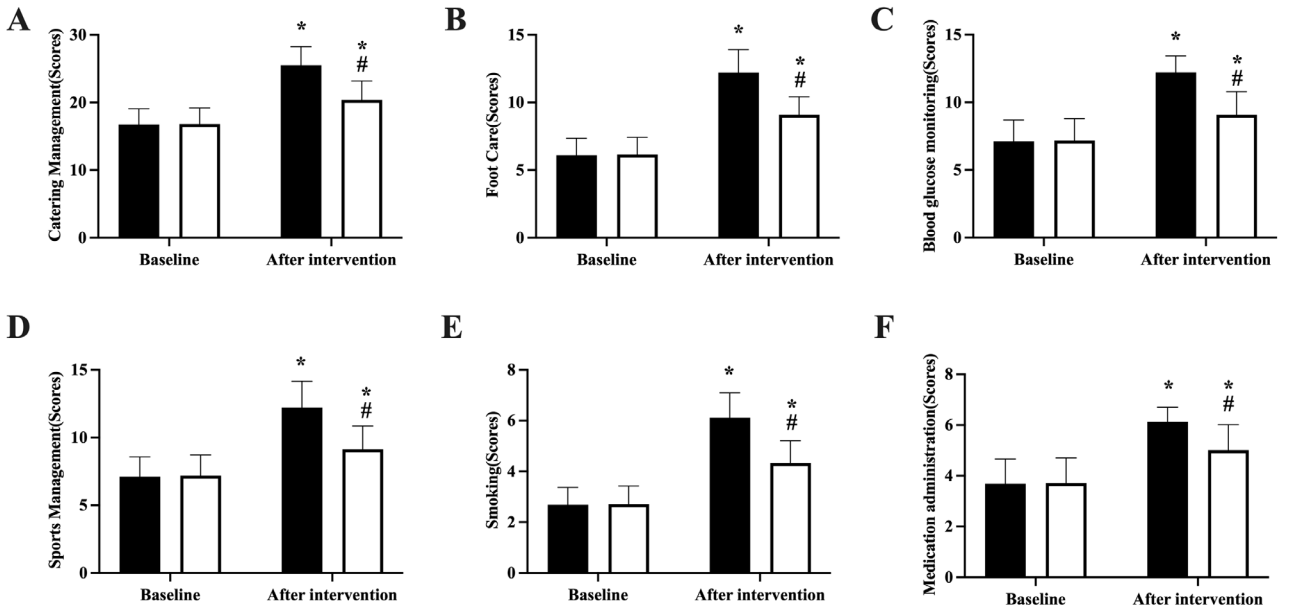

Fig. 3: Comparison of self-management scores between the two groups, (A): Comparison of dietary management; (B): Comparison of foot care; (C): Comparison of blood glucose monitoring; (D): Comparison of exercise management; (E): Comparison of smoking and (F): Comparison of medication management
Note: (■): CBT group and (▭): Control group

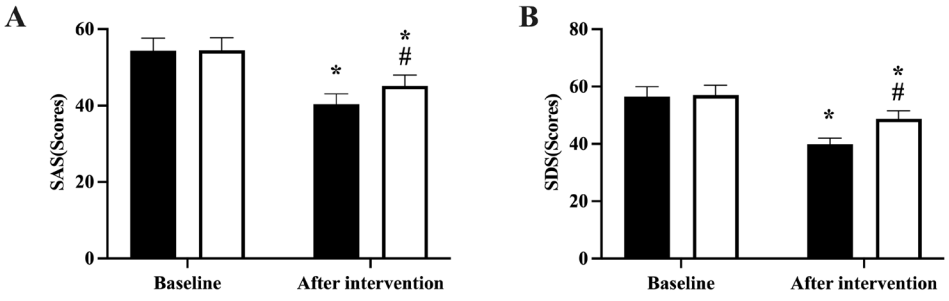

Fig. 4: Comparison of anxiety and depression scores between the two groups, (A): Comparison of SAS and (B): Comparison of SDS
Note: (■): CBT group and (▭): Control group

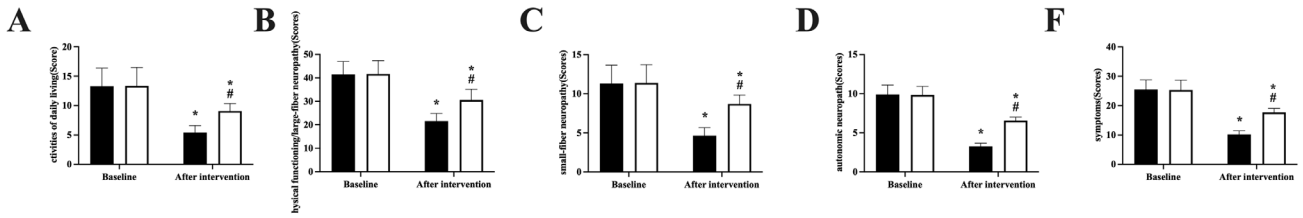

Fig. 5: Comparison of quality of life scores between the two groups, (A): Activities of daily living comparison; (B): Physical functioning/large-fiber neuropathy comparison; (C): Small-fiber neuropathy comparison; (D): Autonomic neuropath comparison and (E): Comparison of symptoms
Note: (■): CBT group and (▭): Control group

LUAD stands as one of the most widespread malignancies worldwide, distinguished by swift proliferation and invasive metastasis, and ranks among the major causes of cancer-correlated mortality[17]. GEM, an artificial pyrimidine nucleoside analog introduced to the market in 1996 in the United States, falls under the category of cell cycle ancillary drugs. Its primary mechanism of action involves targeting the DNA post-synthetic phase and late G1 phase, obstructing cell progression from the G1 to the S phase, and suppressing DNA elongation. Additionally, it can interfere with the self-repair mechanisms of DNA chains through unique masking chains, prevent RNA synthesis, and trigger cell apoptosis, hence displaying its anti-cancer function[18]. Multiple antecedent investigations have attested to the efficacy of GEM as a potent first-line therapeutic agent in combatting diverse malignancies, encompassing NSCLC [19-22]. Nevertheless, the primary mechanism underlying GEM's actions remains poorly understood. Thus, this research sought to delve into this aspect. The findings of this study demonstrated that GEM effectively dampened the proliferation, migration, invasion, and EMT of A549 and PC-9 by repressing the JAK/STAT3 signaling pathway, thereby exhibiting anti-tumor effects.

Cell apoptosis is a critical physiological process. The balance between apoptosis and proliferation is of paramount significance to maintaining cellular homeostasis[23]. EMT serves as an essential procedure in cancer metastatic development, involving the acquisition of mesenchymal characteristics by epithelial cells, leading to enhanced cell motility and migratory capacity[24]. Cell apoptosis, proliferation, and metastasis are the main hallmarks of cancer, possibly directly contributing to tumor proliferation and subsequent malignant behaviors. Consequently, numerous drugs function by facilitating cell apoptosis and suppressing cell proliferation and EMT transformation to exert their anti-cancer effects. Here, our study delved into the influence of GEM on apoptosis, proliferation, and metastasis in A549 and PC-9. As evidenced by our experimental data, GEM impeded cell proliferation, migration, and invasion, while elevating BAX, E-cadherin, and C-caspase profiles, as well as attenuating Bcl-2, vimentin, and N-cadherin profiles. All these phenomena highlighted GEM's anti-cancer role in LUAD.

The JAK/STAT3 signaling pathway exerts a critical function in modulating physiological processes in normal cells.

Nonetheless, in tumor cells, the JAK/STAT3 pathway frequently experiences excessive activation, leading to aberrant processes such as cell proliferation, invasion, metastasis, and inflammatory responses[15]. This abnormal activation may be attributed to tumor development, progression, and therapy resistance. For instance, propofol vigorously curbs proliferation, invasion, and migration, and elicits apoptosis in ES-3 and Osteoclast-Associated Receptor (OSCAR)-2 cells by down-regulating HOST2 and impeding JAK2/STAT3 pathway activation[25]. Additionally, JAK/STAT3 pathway activation is implicated in the development of liver cancer[26], cervical cancer[27], prostate cancer[28], and thyroid cancer[29]. More of note, proanthocyanidins exhibit the capability to quell the malignant advancement of NSCLC cells *via* JAK2/STAT3 pathway suppression[30]. Thus, drugs can hinder cancer progression by inhibition of the JAK/STAT3 pathway. Nonetheless, the function of GEM and JAK/STAT3 in LUAD remains ambiguous.

Here, the experiments of qRT-PCR and Western blot ascertained JAK/STAT3 pathway profile in cells. We discovered that the JAK/STAT3 pathway displayed a high profile in A549 and PC-9. Moreover, GEM curbed the cells' proliferation, invasion, migration, and EMT processes but bolstered their apoptosis through JAK/STAT3 pathway inhibition. This finding underscores the pivotal role of the JAK/STAT3 pathway in LUAD. Suppressing JAK or STAT3 activation can disrupt abnormal JAK/STAT3 signaling transduction, thereby curbing tumor cell proliferation, modulating cell apoptosis, mitigating inflammatory responses, and potentially yielding therapeutic effects against tumors. This novel and potentially effective cancer treatment strategy warrants further investigation.

To summarize, our research has corroborated that GEM can exert an anti-tumor function by curbing the JAK/STAT3 pathway and suppressing A549 and PC-9 cell proliferation, invasion, migration, and EMT processes. These findings provide a significant theoretical foundation for the development and clinical application of GEM as a lung cancer therapeutic agent. Nevertheless, this study also has inherent limitations that must be

acknowledged. Firstly, it mainly relies on cellular experiments and lacks support from *in vivo* animal studies and clinical trials. Secondly, while this study has primarily explored the mechanisms underlying GEM's impact on the JAK/STAT3 pathway, its interactions with other signaling pathways remain unexplored and necessitate further investigation.

Conflict of interests:

The authors declared no conflict of interests.

REFERENCES

1. Siegel RL, Miller KD, Jemal A. Cancer statistics, 2019. CA Cancer J Clin 2019;69(1):7-34.
2. Devarakonda S, Morgensztern D, Govindan R. Genomic alterations in lung adenocarcinoma. Lancet Oncol 2015;16(7):342-51.
3. Ruiz-Cordero R, Devine WP. Targeted therapy and checkpoint immunotherapy in lung cancer. Surg Pathol Clin 2020;13(1):17-33.
4. Rana M, Perotti A, Bisset LM, Smith JD, Lamden E, Khan Z, *et al.* A ferrocene-containing nucleoside analogue targets DNA replication in pancreatic cancer cells. Metallomics 2022;14(7):mfac041.
5. Ewald B, Sampath D, Plunkett W. H2AX phosphorylation marks gemcitabine-induced stalled replication forks and their collapse upon S-phase checkpoint abrogation. Mol Cancer Ther 2007;6(4):1239-48.
6. Sarvepalli D, Rashid MU, Rahman AU, Ullah W, Hussain I, Hasan B, *et al.* Gemcitabine: A review of chemoresistance in pancreatic cancer. Crit Rev Oncog 2019;24(2):199-212.
7. Shelley MD, Jones G, Cleves A, Wilt TJ, Mason MD, Kynaston HG. Intravesical gemcitabine therapy for Non-Muscle Invasive Bladder Cancer (NMIBC): A systematic review. BJU Int 2012;109(4):496-505.
8. Wu Y, Tao L, Liang J, Qiao Y, Liu W, Yu H, *et al.* miR-187-3p increases gemcitabine sensitivity in breast cancer cells by targeting FGF9 expression. Exp Ther Med 2020;20(2):952-60.
9. He H, Liang L, Huang J, Jiang S, Liu Y, Sun X, *et al.* KIF20A is associated with clinical prognosis and synergistic effect of gemcitabine combined with ferroptosis inducer in lung adenocarcinoma. Front Pharmacol 2022;13:1007429.
10. Mengie Ayele T, Tilahun Muche Z, Behaile Teklemariam A, Bogale Kassie A, Chekol Abebe E. Role of JAK2/STAT3 signaling pathway in the tumorigenesis, chemotherapy resistance, and treatment of solid tumors: A systemic review. J Inflamm Res 2022;15:1349-64.
11. Huang B, Lang X, Li X. The role of IL-6/JAK2/STAT3 signaling pathway in cancers. Front Oncol 2022;12:1023177.
12. Loh CY, Arya A, Naema AF, Wong WF, Sethi G, Looi CY. Signal Transducer and Activator of Transcription (STATs) proteins in cancer and inflammation: Functions and therapeutic implication. Front Oncol 2019;9:48.
13. Lee H, Jeong AJ, Ye SK. Highlighted STAT3 as a potential drug target for cancer therapy. BMB Rep 2019;52(7):415-23.
14. Liu Y, Liao S, Bennett S, Tang H, Song D, Wood D, *et al.* STAT3 and its targeting inhibitors in osteosarcoma. Cell Prolif 2021;54(2):e12974.
15. Jin W. Role of JAK/STAT3 signaling in the regulation of metastasis, the transition of cancer stem cells, and chemoresistance of cancer by epithelial–mesenchymal transition. Cells 2020;9(1):217.
16. Puigdevall L, Michiels C, Stewardson C, Dumoutier L. JAK/STAT: Why choose a classical or an alternative pathway when you can have both? J Cell Mol Med 2022;26(7):1865-75.
17. Inamura K. Clinicopathological characteristics and mutations driving development of early lung adenocarcinoma: Tumor initiation and progression. Int J Mol Sci 2018;19(4):1259.
18. Pandit B, Royzen M. Recent development of prodrugs of gemcitabine. Genes 2022;13(3):466.
19. Jiang X, Ma Y, Wang T, Zhou H, Wang K, Shi W, *et al.* Targeting UBE2T potentiates gemcitabine efficacy in pancreatic cancer by regulating pyrimidine metabolism and replication stress. Gastroenterology 2023;164(7):1232-47.
20. Wang R, Gao D, Chen C, Fan G, Cheng H, Tao Y, *et al.* ADAM12 promotes gemcitabine resistance by activating EGFR signaling pathway and induces EMT in bladder cancer. Clin Transl Oncol 2023;25(5):1425-35.
21. Hindson J. Gemcitabine and cisplatin plus immunotherapy in advanced biliary tract cancer: A phase II study. Nat Rev Gastroenterol Hepatol 2022;19(5):280.
22. Lv P, Liu M. Meta-analysis of the clinical effect of Kanglaite injection-assisted gemcitabine plus cisplatin regimen on non-small cell lung cancer. Am J Transl Res 2023;15(5):2999-3012.
23. Loftus LV, Amend SR, Pienta KJ. Interplay between cell death and cell proliferation reveals new strategies for cancer therapy. Int J Mol Sci 2022;23(9):4723.
24. Cho ES, Kang HE, Kim NH, Yook JI. Therapeutic implications of cancer Epithelial-Mesenchymal Transition (EMT). Arch Pharm Res 2019;42(1):14-24.
25. Shen X, Wang D, Chen X, Peng J. Propofol inhibits proliferation, migration, invasion and promotes apoptosis by regulating HOST2/JAK2/STAT3 signaling pathway in ovarian cancer cells. Cytotechnology 2021;73(2):243-52.
26. Xiao Y, Li Y, Shi D, Wang X, Dai S, Yang M, *et al.* MEX3C-mediated decay of SOCS3 mRNA promotes JAK2/STAT3 signaling to facilitate metastasis in hepatocellular carcinoma. Cancer Res 2022;82(22):4191-205.
27. Bai Y, Li H, Lv R. Interleukin-17 activates JAK2/STAT3, PI3K/Akt and nuclear factor-κB signaling pathway to promote the tumorigenesis of cervical cancer. Exp Ther Med 2021;22(5):1291.
28. Chen L, Wang Y, Zhang B. Hypermethylation in the promoter region inhibits AJAP1 expression and activates the JAK/STAT pathway to promote prostate cancer cell migration and stem cell sphere formation. Pathol Res Pract 2023;241:154224.
29. Liu W, Wang X, Wang L, Mei Y, Yun Y, Yao X, *et al.* Oridonin represses epithelial-mesenchymal transition and angiogenesis of thyroid cancer *via* downregulating JAK2/STAT3 signaling. Int J Med Sci 2022;19(6):965-74.

30. Wu Y, Liu C, Niu Y, Xia J, Fan L, Wu Y, *et al.* Procyanidins mediates antineoplastic effects against non-small cell lung cancer *via* the JAK2/STAT3 pathway. Transl Cancer Res 2021;10(5):2023-35.

This article was originally published in a special issue, "Exploring the Role of Biomedicine in Pharmaceutical Sciences" Indian J Pharm Sci 2024:86(1) Spl Issue "244-252"